Automated Generation of Railway Track Geometric Digital Twins (RailGDT) from Airborne LiDAR Data

Ariyachandra M.R.M.F., Brilakis I.
University of Cambridge, United Kingdom
mfa47@cam.ac.uk

Abstract. Automated generation of railway track geometric digital twins (RailGDT) from airborne LiDAR data is an unresolved problem. Currently, this onerous manual procedure counteracts the expected benefits of the resulting RailGDT. State-of-the-art methods provided promising results, but are unable to generate RailGDTs over kilometres with complex railway geometries without forfeiting precision and manual cost. The challenge that this paper address is how to efficiently minimise manual cost for generating RailGDTs such that the benefits provide even greater compared to the initial investment in RailGDTs. We tackle this challenge by leveraging the highly standardised nature of railways. The method restricts the search region and segments track elements given their locations relative to masts, using an extended RANSAC algorithm. Next, it converges segmented point clusters with various pre-assembled track element profiles to obtain RailGDTs. Experiments on 18 km datasets yield 95% and 98% average F1 scores for rail and trackbed point cluster segmentation. The RailGDT accuracy is 3.4 cm and 2.7 cm RMSEs for rails and trackbeds.

1. Introduction

A Digital Twin (DT) is a digital copy of a real-world asset (i.e. building, railway, bridge) that is based on massive, cumulative, real-time, real-world data measurements in multiple dimensions (Buckley and Logan, 2017). We use the term 'geometric DT' (GDT) to define the fundamental 3D geometry, without which many DT applications do not exist. A GDT is generated using raw spatial data, [i.e. Point Cloud Datasets (PCD)s] collected with laser scanners. This is beneficial for rail inspection maintenance and practices, which usually require substantial costs and timescales. The method given in this paper is a part of a much larger framework for twinning railways which contains three phases. The 1st phase is the automated removal of noise points and mast segmentation (Ariyachandra and Brilakis, 2020a). The 2nd phase is the generation of Overhead Line Equipment (OLE) GDTs (Ariyachandra and Brilakis, 2020b) and the 3rd phase is the generation of railway track geometric digital twins (RailGDT), which is the scope of this paper. Railway track refers to rails and trackbed, which represent the most critical elements in railway track structure (Dvořák *et al.*, 2017).

Railways are complicated, safety-critical systems (Wilson *et al.*, 2007) that occasionally face catastrophic risks such as derailments and collisions (European Railway Agency, 2020). While these incidents are considered to be rare, the total costs of railway accidents are estimated at £3.4 billion in 2018 (European Railway Agency, 2020). Maintenance, safety management and retrofitting are therefore vital operations in the life-cycle of existing rail infrastructure. Yet, European and UK rail industries are partly built on antiquated legacy systems that are becoming more difficult to maintain. The railway system in the UK is the oldest in the world (Lee, 1945) and comprised of a patchwork of overlapping designs built at different times (RailEngineer, 2020). Current maintenance processes can no longer cope with the increasing complexity of modern complex socio-technical systems (Zio, 2018) due to the absence of Information and Communication Technology (ICT) sector-level data management. This explains why there is a huge market demand for less labour-intensive railway maintenance techniques that can efficiently boost railway operations and productivity. Industry experts believe that the wider adoption of DTs will unlock 15-25% savings to the global infrastructure market by 2025

(Gerbert *et al.*, 2016). The use of a DT is greatest during the design stage, while little use is made in the closeout stage, and almost absent in the maintenance stage (Buckley and Logan, 2017). Our DT focus is on the latter, except as otherwise noted. The adoption of RailGDTs is very limited. Soni (2016) reported that the total time to reconstruct the GDT of 0.5 m length track section using PCDs was between 20-40 minutes. Every DT generation hour saved can prevent critical failures or accidents so that continuous operations of railways can be achieved without impeding the national economy (Rail Delivery Group, 2014).

This paper only focuses on generating 3D models that correspond to LODs which can be achieved through laser scanning technology. Thus, the proposed method in this paper generates RailGDTs in LOD 300, that are in line with the End-User Requirements (EUR)s namely; (1) EUR 1: component-level digital representation which includes the main structural component types of a sensed asset with a component-level resolution (Sacks et al., 2017), (2) EUR 2: component's explicit geometry representation and property sets (Borrmann and Berkhahn, 2018), (3) EUR 3: component's taxonomy by labelling their element types (Koch and Konig, 2018) and (4) EUR 4: all above-listed EURs in a platform-neutral data format, such as Industry Foundation Classes (IFC) (Koch and Konig, 2018).

Leading software vendors such as Autodesk, Bentley, Trimble, AVEVA and ClearEdge3D provide advanced commercial twinning solutions. Yet the automation provided by these software packages is tailored only to generic or pre-defined geometries; it is still far from being fully automatic (Agapaki and Brilakis, 2018). For instance, OpenRail Designer has a certain degree of automation by combining survey, design rules, and operational requirements to generate optimal geometry of the track on a 2D plane (Bentley Systems, 2018). However, it's shape-creation method focuses only on continuous structures belonging to the alignment. The lack of interoperability between the existing software makes the modelling process challenging (Kenley et al., 2016). Other commercial applications cannot fully automate any one of the EURs. We investigated the current railway twinning process using existing software packages for the whole framework mentioned at the beginning of this paper (Ariyachandra and Brilakis, 2019). Our results illustrate that the 'bottlenecks' of digital twinning using current software applications are (1) existing software can semi-automatically extract generic shapes in PCDs. Yet, their ability to extract non-generic shapes is limited and is laborious. Vegetation overlap adds extensive labour hours, (2) the occlusions, data gaps and varying point density slows down the workflow and add hours of adjustments, (3) EURs 1, 3, & 4 can only be manually achieved, (4) there is no single software that can offer a one-stop GDT generation solution.

2. Research Background

We review the existing research methods by dividing them into two parts namely, (1) object segmentation in PCDs and (2) 3D model fitting to segmented point clusters. The point cluster segmentation step delivers labelled point clusters corresponding to track elements (i.e. rail #1, trackbed #2). Model fitting elaborates the methods for representing the 3D geometry of the segmented point clusters in an object-oriented data format (i.e. IFC).

Jwa and Sonh (2015) used Kalman filter-based railway tracking, which approximated the orientation of the rail track trajectory and then segmented track region and railhead points using a Bayesian decision process and a region growing approach. However, the threshold parameters are appropriate only for relatively simple datasets without any switches, bridges, and train stations. Gézero and Antunes (2019), used the scan angle value of the Mobile Laser Scanned (MLS) data to segment rail points. This method was sensitive to the colour information and the scan angle value of the PCD, hence, does not work for mono-colour PCDs. Moreover, it is valid

only for straight rail tracks without any slopes and not a fully automated solution for the segmentation of rails. Yang and Fang (2014) employed a moving window filtering operator to analyse elevation patterns in points along MLS scanning lines to segment track structure element points. However, the method was less accurate in extracting forking junctions due to the complexity of track geometry. Lou et al. (2018) addressed some of the above limitations using MLS profile information such as position, velocity, and altitude. Their method is sensitive to the density of their input PCD, hence, do not work well for different input PCDs. Niina et al. (2018) proposed a method that initially clipped the PCD of the rail track and projected those points on the section perpendicular to the rail track position using the trajectory of the MLS scanner. Next, the method localised the position of the gauge corner, by matching the shape of the ideal railhead to the projected points. The method proposed by Sánchez-Rodríguez et al. (2018), used the MLS scanner profile information and a saliency map to classify ground points. They localised rails, curbs and other ground elements with a peak detection algorithm. All the aforesaid methods are highly dependent on MLS scanner profile information. The ALS are unorganised as they do not contain any scanner profile information such as the trajectory of the scanner or scan angle values. Thus, the above methods are ineffective for ALS PCD. The existing methods can segment rail track points without using scanner profile information as proposed by Oude Elberink et al. (2013). The method initially analysed the height distribution of the points using a digital terrain model (DTM). They analysed all points within 0.5 m above DTM height for rail segmentation using the RANSAC algorithm, assuming that the majority of the roughly segmented rail points within a grid cell fit one line within a certain buffer (0.05 m). However, this method was highly dependent on the determination of DTM height, which was sensitive to the density of their PCD. The method is proven to be effective only for small lengths (typically 300 m) and relatively simple datasets without any switches, bridges, and train stations. The method proposed by Jeon and Kim (2019), used contact cable positions (Jeon and Choi, 2013) as references to segment rail tracks, following the same approach developed by Oude Elberink et al. (2013). However, they assumed that rails are straight lines hence this method cannot be used for curved rail tracks. Both of these methods highly rely upon the segmentation of cables. The sparseness of data on foreground elements in railways is expected due to the small size of the cables in relation to the size of the rail track, and likely to occur despite the scanning technology. It creates obstacles that hinder the robustness of cable segmentation as explained before (Ariyachandra and Brilakis, 2020b). These factors reduce the potential performance of the methods discussed in Jeon and Kim (2019) and Oude Elberink et al. (2013) for lengthier datasets. Cheng et al. (2019) proposed a method that segmented track elements with an elevation and 3D local spherical neighbourhood analysis. The method was sensitive to PCD densities and numbers of points in a particular interval; hence it is dubious that this method is suitable for varying densities of input PCD. Some of the parameters were sensitive to the scan angular resolution of the terrestrial laser scanner (TLS). Thus, this method is incompatible with ALS data, as they do not contain any profile information.

Arastounia and Oude Elberink (2016) proposed an approach to segment trackbed points based on the statistical method of the global map. The height difference of the trackbed was small in their input PCD. Therefore, the method calculated the standard deviation in the fixed neighbourhood to obtain a threshold to distinguish the trackbed from other targets. Their input PCD did not contain any large slopes hence, they assumed that the height difference between points remained constant. A similar approach in Pastucha (2016) used MLS trajectory to limit the search area of the trackbed. This method could effectively reduce the amount of the search calculations but it could not provide a uniform threshold for railway corridors in different scenarios. Both aforementioned methods assume that trackbeds are relatively flat. Subsequently, the geometry and elevation features of the track beds made it easy to recognise. Also, these methods require large-scale neighbourhood computation and hence do not work

well with real-world scenarios. The real-world railway corridors typically contain vertical elevations span over kilometres hence the above methods are not fit for purpose. Yang and Fang (2014) extracted track beds by analysing spatial patterns on MLS scanning lines. Methods proposed in Lou et al. (2018) and Gézero and Antunes (2019) used scan angle value of MLS data to segment trackbed. In Gézero and Antunes (2019), their method only indicated the mere existence of the trackbed boundaries by extracting top and bottom track bed lines and did not segment point clusters of trackbeds. However, in real-world railways, the trackbed width changes due to the varying horizontal elevation and consequently, the scan angle of the PCD points representing the top and bottom ballast break-lines, will also change. Also, the above-mentioned methods are highly dependent on the geometric patterns and the reflectance characteristics of MLS railway PCD.

The choice of the fitting technique mainly depends on the nature of the object, the modelling approach, and the application scenario where the object needed to be modelled. Implicit representation represents the 3D shape of the objects using mathematical (implicit) functions. Common implicit functions can use to define point segments as planes (Limberger and Oliveira, 2015), spheres, and toruses (Schnabel *et al.*, 2007), among others. These functions can describe few primitives only; therefore, have a very limited usage when describing non-primitives of railway elements such as trackbeds. A model can be described using Boundary Representation (B-rep) by exploiting the information about vertices, edges, loops, and the way of assembling them to form the object. The primitive shapes in construction sites, indoor planer objects, and synthetic building PCDs have been represented using B-rep methods (Oesau *et al.*, 2014; Valero and Cerrada, 2012) yet these methods could hardly smooth the point regions in railway elements when occlusions and data gaps are present. Constructive Solid Geometry (CSG) methods contain information about how an object was constructed and simultaneously functioned as a shape representation method (Deng *et al.*, 2016). CSG methods reconstructed the 3D shape of piping systems (Patil *et al.*, 2017), kitchen objects (Rusu *et al.*, 2008), and indoor environments (Xiao and Furukawa, 2012). Well-designed and complex CSG modelling strategies are needed to model non-primitives of track elements. Another most commonly used method is Swept Solid Representation (SSR), which exploits the 2D cross-sectional profile of the element to represent the volumetric characteristics of the 3D shape, by sweeping it along a defined path in the 3rd dimension. The use of this technique can be found in state-of-the-art methods in indoor environments for building elements (Budroni and Boehm, 2010), steel beams (Laefer and Truong-hong, 2017) and bridge components (Lu and Brilakis, 2020). Its implementation for railway masts and railway OLE elements can be found in our previous work (Ariyachandra and Brilakis, 2020b, 2021). This paper will investigate its implementation for track elements.

The review provided in the previous section demonstrates that the problem of generating RailGDTs automatically from railway ALS data has yet to be solved. The limitations in each method reduce their robustness thus unable to provide the expected automation over kilometres on the ground. We propose a method for automated RailGDT generation, aiming to meet objective 1: automatically segment track structure elements as labelled point clusters and objective 2: automatically reconstruct the 3D geometry of segmented track element point clusters in IFC format. We answer the research questions RQ1: How to automatically segment railway track structure elements in the form of labelled point clusters from real-world railway PCDs with varying horizontal and vertical elevations and complex railway geometries; without using any additional prior information such as neighbourhood structures, scanning geometry and intensity of input data; and where occlusions, data gaps and varying point density exist?; RQ2: How to automatically separate rails from other linear elements adjacent to the railway corridor without relying on prior knowledge and manual inputs?; and RQ3: How to automatically reconstruct labelled point clusters into 3D IFC objects for the railway domain?.

3. Proposed Solution

We hypothesize that the use of railway topology has the theoretical potential to perform better when segmenting and modelling the geometry of railway elements in PCDs with varying geometric patterns. We have tested this hypothesis with three approximately 6 km (total 18 km) long PCDs (Dataset A, B, and C) obtained from the track located between 's-Hertogenbosch and Nijmegen in the Netherlands. Railways are a linear asset type; their geometric relations remain roughly unchanged, often over very long distances. Close inspection of railway PCDs validates this effect, with repeating geometrical features such as, (1) the geometric relationships among railway elements (i.e. masts, cables, and rails) remaining fairly unchanged along the railway corridor (Network Rail, 2018), (2) the connections between masts and cables are placed in regular intervals (60 m intervals on average), (3) the main axis of the railway masts (Z-axis) is roughly perpendicular to the rail track direction (X-axis) [error tolerance is 11° (Network Rail, 2018)] and (4) masts are always positioned as pairs throughout the rail track. We use these four geometric features as assumptions for the proposed method. The method is designed to twin only the typical double-track railways because they make up 70% of the existing and under-construction railway network in the UK and Europe (Eurostat 2019). The method given in this paper is a part of a railway twinning framework as described in the introduction. Hence, inputs of the method in this paper are (1) railway corridor PCD, (2) ground truth mast position coordinates (RM_{Cor}). The ground truth is used, to evaluate the method on its own without adding the error of the segmented mast predictions of the 1st phase (Ariyachandra and Brilakis, 2020a). The outputs of this paper are (1) labelled point clusters of track elements and (2) RailGDTs in .ifc format. Figure 1 illustrates the workflow of the proposed methodology.

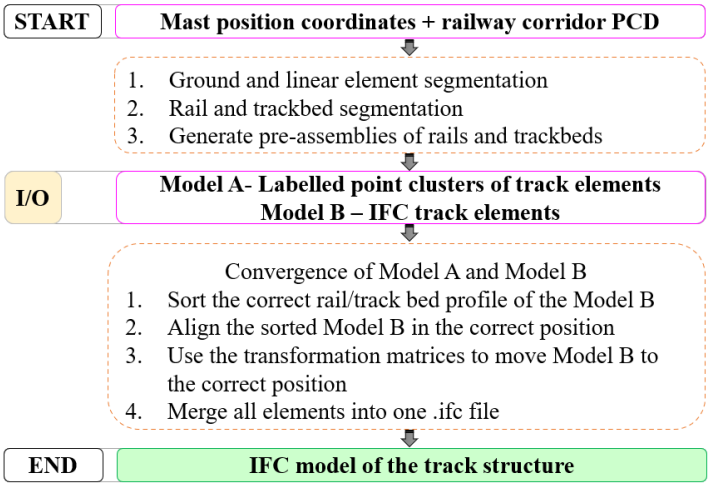

Figure 1: Workflow of the proposed method

The first step is to separate the ground points including horizontal and quasi-horizontal planes from the ALS data. This is an essential and advantageous step because; (1) it permits segmenting points associated with rails and track beds from the railway PCD, (2) it allows one to easily exploit the linearity of rails against the ground using linear feature extraction algorithms, (3) it minimises the effect of false positives that may arise due to other linear elements such as OLE cables in the railway ALS data, and finally (4) it significantly reduces the number of points required for the rail and trackbed segmentation method, leading to faster computational performance. Initially, we use the RANSAC plane detection algorithm to segment point clusters of the horizontal and quasi-horizontal ground planes. A pre-processing step is used before the RANSAC algorithm that divides the PCD into sub boxes, using a crop box filter (CBF). The selected crop box [Crop Box 1 (CB_1)] ensures that only two consecutive pairs of masts fall in each CB_1 (60 m on average). This CBF automatically extracts all the data

within a given box, and hence simplifies the cloud by increasing the speed of RANSAC due to the small number of points considered each time. This further removes any noise data that contain vegetation and other rail infrastructure built adjacent to the track. The method computes the minimum and the maximum points of CB_1 using the $RM_{Cor}$of two consecutive pairs of masts. Next, we apply the RANSAC plane detection algorithm for each CB_1. RANSAC algorithm iteratively and randomly sample points to estimate the hypothesis plane and then tests the plane against the remainder of the PCD. We set the parameters of RANSAC plane detection to extract planes that satisfy the steepest incline that exists in the UK railways (*Gradients of the British Main Line Railways*, 2016). A closer observation of the resulting data demonstrates that these horizontal and quasi-horizontal planes contain points associated with rails and trackbeds as well as a few unrelated points. This is because the position and the orientation of a raw railway PCD are not always properly aligned or paralleled to the global axes. In Ariyachandra and Brilakis (2020a), we used PCA to align a railway such that the global X-axis and the horizontal alignment of the input PCD in this study are now roughly paralleled to the global axes. Yet, the alignment is not perfect mainly because PCA provides only a rough estimate and the railway corridor itself contains a certain degree of curvature and slope. As a result, CB_1s are rotated in different directions around the Z-axis. Hence, we calculate the tangent between the resulting and optimum CB_1s to compute the rotation [arctangent (atan2)] around Z-axis and thereby align each CB_1 along the track direction (Eq. 1);

$$atan2(Y,X) = \left\{\arctan\frac{Y_{max} - Y_{min}}{X_{max} - X_{min}}\right\} \quad \text{Eq. 1}$$

Where, $X_{max}, Y_{max}, X_{min}$ and Y_{min} represent the maximum and minimum XY coordinates, respectively, sorted from one pair of masts. The method automatically applies this rotation to each CB_1, and then uses CBF to extract horizontal and quasi-horizontal planes inside a given CB_1. We then use a method to segment rails and track beds from the resulting CB_1s based on an extended RANSAC line detection method. We hypothesise that the only linear element on CB_1 PCD now represents rails, while the rest of the points on CB_1 represent track bed points. The previously calculated CB_1 are now aligned along the track direction; yet, it is difficult to segment rail tracks parallel to the track direction, if there is a curvature occurred within any CB_1. Thus, we automatically segment each CB_1 such that the resulting pieces [Crop Box 2 (CB_2)] are relatively straight enough to segment linear elements parallel to track direction. This step also reduces computational time by processing a segment of CB_2 at a time. It creates 8 CB_2s between a set of two consecutive mast pairs that represent near straight pieces of railway PCD and repeats for the next pairs of masts throughout the track (Figure 2).

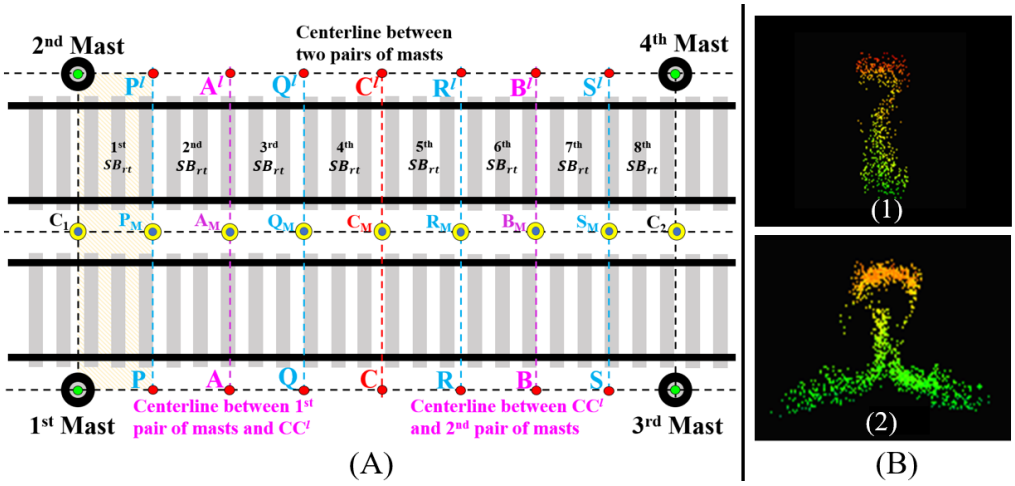

Figure 2: (A) Segmentation step, (B1) Segmented rail, (B2) Segmented rail improved with radius neighbour search

We use a pre-processing step that allows projecting slopes on the rail tracks on to the ground, such that the RANSAC can segment those rails as lines parallel to rail track direction despite their vertical elevations/inclines. Using RANSAC, four lines, which represents four rails in a double-track railway, with maximum inliers are then iteratively generated by determining the most probable hypothesis line for each CB_2. We observed that the resulting four lines do not contain all the points of the rail point cluster (Figure 2B1). Hence, we use a radius neighbour search to include any missing points during RANSAC detection. For a given segmented line of P points (Eq. 2);

$$P = \{p_1, \ldots, p_N\}, p_i \in \mathbb{R}^3 \quad \text{Eq. 2}$$

We find all the neighbour points of the segmented lines N such that (Eq. 3);

$$N(q, r) = \{p \in P \} | \, \|p - q\| < r\} \quad \text{Eq. 3}$$

inside a radius $r \in \mathbb{R}^3$ of a query point $r \in \mathbb{R}^3$. We set radius (r) to 0.1 m and this parameter is fine-tuned with experimental results to ensure that only rail points fall in each neighbourhood. (Graphs representing calculations for the parameters are not illustrated due to limited space). We used a regular space portioning; the octree to accelerate the neighbour search in the PCD. The resulting segmented points now consist of rail point clusters including the missing points in the previous stage (Figure 2B). We use the performance matrices to measure the performance of step 2 as expressed below (Eq. 4, Eq. 5, 6). We observe that the segmented linear elements at this stage represent both rails and other linear elements along the rail track direction in railway PCDs. As a result, the segmentation performance reached a precision of 91.7%, a recall of 94.4%, and an F1 score of 93.1% (Table 1). False positives in these numbers include other linear elements such as walls, fences adjacent to the track, lines segmented on the trackbed and ground, among others.

$$Precision = \frac{Correctly\ \ segmented\ rail\ tracks\ (TP)}{Total\ segmented\ linear\ elements\ (TP + FP)} \quad \text{Eq. 4}$$

$$Recall = \frac{Correctly\ \ segmented\ rail\ tracks\ (TP)}{Total\ number\ of\ rail\ tracks\ (TP + FN)} \qquad F1\ Score = \ 2\ x\ \frac{Precision\ x\ Recall}{Precision + Recall} \quad \text{Eq. 5, 6}$$

A closer observation of the railway PCD shows that (1) the number of points per other linear elements such as walls, fences are considerably higher than those of the rails; (2) the number of points per other linear elements such as lines on the trackbed and ground are considerably lower than those of the rails. These observations are expected despite the density of the input PCD, which likely to occur regardless of the scanning technology used. Therefore, we hypothesis that the number of points per each rail should not drastically vary as the geometric properties of the rails are consistent throughout the whole PCD. Hence, we use a point-based calculation method to differentiate point clusters of rails from other linear elements. Initially, we experimentally define a threshold D_1, by calculating the ratio between the number of points per other liner elements such as walls and fences over the number of points per rail point cluster along the track direction. We obtained the optimum D_1 as 2.12 for all the datasets by computing precision, recall, and F1 score for different D_1 values. For the segmented point clusters, we compute the number of points of the 1st segmented line and repeat the same for the next optimum subset of points, i.e., the 2nd line, that is chosen by RANSAC. Next, we calculate D_1 of these two lines and true positive lines that represented by $\widehat{K}$; where, D_k is the ratio between the point counts of the 1st and 2nd lines.

$$\widehat{K} = \begin{cases} 1 & D_k \leq D_1;\ true\ positive \\ 0 & otherwise;\ false\ positive \end{cases} \quad \text{Eq. 7}$$

We filter the lines using Eq. 7. We replicate this procedure until there are 4 lines per CB_2 (as there are 4 rails in a double-track railway) and repeat for next CB_2 s throughout the track. This step increased the precision, recall, and F1 score up to 93.2%, 95.4%, and 94.3%, respectively (Table 1). Yet, the segmented linear elements still represent both rails and other linear elements

along the rail track direction such as lines on trackbed and ground that contain a smaller number of points per element compared to the rails. Next, we experimentally define a threshold D_2 to filter false positives of lines on the trackbed and ground. This threshold is obtained by calculating the ratio between the number of points per rail point cluster over the number of points per other liner elements such as lines on the trackbed and ground along the track direction. We obtain the optimum D_2 = 1.7 by computing precision, recall and F1 score for different D_2 values. We compute D_2 of these two lines and true positive lines that represented by $\widehat{M}$; where, D_m is the ratio between the point count of the previous line over the point count of the current line. We filter lines using Eq. 8. This procedure only loops over the first 4 lines chosen by RANSAC. The linear elements with higher points counts are already discarded at the 1st step. Hence, we only need to remove linear elements with lower point counts compared to rails to minimise the false positives at this stage.

$$\widehat{M} = \begin{Bmatrix} 1 & D_m \leq D_2; true\ positive \\ 0 & otherwise;\ false\ positive \end{Bmatrix} \quad \text{Eq. 9}$$

The 2nd step increased the precision, recall, and F1 score up to 95.6%, 94.2%, and 94.9%, respectively (Table 1). We initially hypothesised that the points on CB_1 PCD represent rails and track beds only. Hence, once we removed the segmented rail point clusters from CB_1 PCD, the rest of the points in CB_1 PCD is the trackbed point cluster. Thus, our proposed method removes the extracted rail point clusters and overwrites the CB_1 PCD, once all the lines are segmented during the RANSAC line segmentation. The resulting CB_1 PCD represents the trackbed point cluster. Our proposed method has a precision of 100.0%, recall of 96.3%, and F1 score of 98.1% for trackbed segmentation (Table 1). Different colours are assigned to each labelled point cluster (i.e. rail #1, trackbed #2) and are hereinafter denoted as 'Model A's (Figure 3). Next, we design pre-assemblies of track structure elements; hereafter known as 'Model B' using standard railway guidelines (Network Rail, 2018) to represent the geometry of the real track structure elements. These models preserve the geometric properties of the elements, such as different web thicknesses, head widths in rail profiles. We have created 10 different rail and 5 different track bed profiles, compatible with EU and UK railway standards (European Commission, 2017; Network Rail, 2018). We define each of the track elements using extruded area solid definition in IFC format. We use the standard cross-sectional dimensions (European Commission, 2017; Network Rail, 2018) to define the 2D area profile for each element. The method takes the extruded distance by computing the length of each segmented point cluster. The method then uses the Iterative closest point (ICP) algorithm to automatically converge Model B to Model A. We set Model A as the reference cloud (R_C); is kept fixed while different profiles of Model B are source clouds (S_C). The method first converts Model B into .pcd files and then these S_C are transformed to find the best match with the R_C by minimising the distance ($RMSD$) between the two (Eq. 10), where T – transformation, for a set of pairs of points C = (s_i , r_j), $s_i \in S_C, r_j \in R_C$.

$$RMSD\ (T\ (S_C), \mu\ (R_C)) = \frac{\sum_C dist\ (r_j, T(s_i))^2}{|C|}, s_i , r_j \in \mathrm{C} \quad \text{Eq. 11}$$

Hence, by using ICP we first sort the correct rail profile or trackbed profile as the correct profile ideally has the minimum sum of squared differences between the coordinates of the target and reference clouds. Once we sorted the correct profile, our method then converges the sorted model to the correct position and finally gives a transformation matrix which provides the corresponding translation vector and rotation matrix of Model B (model) relative to Model A (point cluster). Finally, the method moves the .ifc format of Model B to the correct position using the resulting transformation matrices and finally merges all units (including rail and trackbed sections) into one file to get the final IFC model of the track structure (Figure 3).

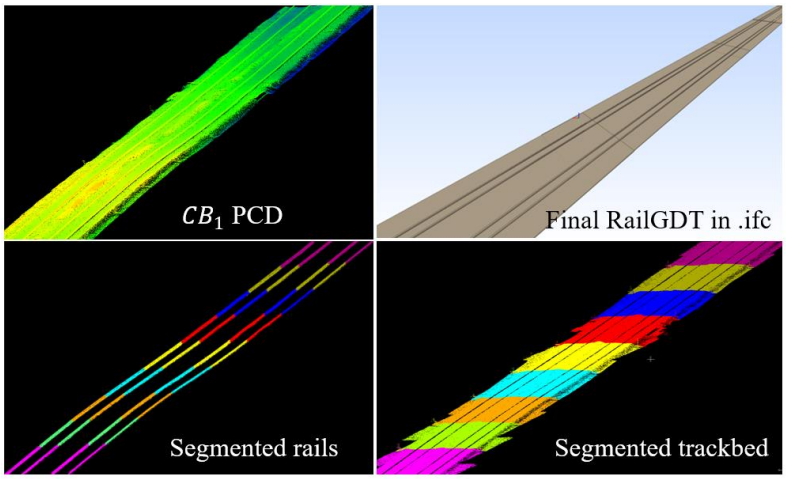

Figure 3: Results of the RailGDT generation

4. Experiments and Evaluation

We manually generated two sets of Ground Truth (GT) datasets consist of three sub-datasets each per one railway PCD; (1) GT A: Manually extracted point clusters of track elements from raw railway PCD. They are used to compare against the automatically detected point clusters of track elements, and (2) GT B: Manually created RailGDTs and used to compare against automated RailGDTs. We implemented the solution with the point cloud library (PCL) version 1.8.0 using C++ on Visual Studio 2017, on a laptop (Intel Core i7-8550U 1.8GHz CPU, 16 GB RAM, Samsung 256GB SSD). We gauged the average segmentation accuracies as explained in section 3 (Table 1).

Table 1: Performance matrices for three datasets

Sequence of steps	Dataset	Precision	Recall	F1 score
Segmentation of rails and other linear elements	A	88.1%	96.5%	92.1%
	B	93.7%	93.0%	93.4%
	C	93.8%	93.6%	93.7%
	Average	91.7%	94.4%	93.1%
Segmentation of rails with 1st refinement	A	91.6%	98.8%	95.0%
	B	93.0%	92.4%	92.7%
	C	95.0%	94.8%	94.9%
	Average	93.2%	95.4%	94.3%
Segmentation of rails with 2nd refinement	A	96.9%	97.8%	97.3%
	B	93.6%	91.6%	92.6%
	C	96.1%	93.1%	94.6%
	Average	95.6%	94.2%	94.9%
Segmentation of the trackbed	A	100.0%	95.8%	97.9%
	B	100.0%	97.8%	98.9%
	C	100.0%	95.6%	97.8%
	Average	100.0%	96.3%	98.1%

We use cloud-to-cloud distance evaluation to detect changes between GT B and the automated ones. Initially, we converted the GT B and the automated GDTs into .pcd files. The evaluation method computed the Root Mean Square Error (RMSE) between each unit of automated GDT of track elements and the corresponding GT B model. The average model distance between the two for all 18 km 3.4 cm RMSE for rails and 2.7 cm RMSE for track beds. The proposed method reduces manual twinning time by 82%. This implies the proposed method outperforms the manual operation.

5. Conclusions

We presented a novel automated method that exploits the highly regulated and standardised railway topology to generate RailGDTs for existing railways from PCD and tested it on an 18 km railway PCDs. Our method does not request any human intervention even though the railway PCDs are highly occluded, sparse, and with varying horizontal and vertical elevations. Based on the high performance delivers, our method; (1) can deal with real-world railway PCD consists of varying track geometries and yet outperforms the existing methods by achieving remarkably high performance; (2) is effective in handling challenges inherited in PCDs such as occlusions, extreme vegetation around the track, and local variable densities of points; (3) provided high-performance matrices despite the different track arrangements such as crossings, turnouts, overbridges and passing loops; (4) offers significant computational cost reductions by automatically cropping a lengthy railway PCD into relatively straight segments. This enables a considerably improved large-scale object detection generally required over kilometres without forfeiting precision and manual cost; and (5) is the first to automatically and robustly solve the RailGDT generation by exploiting reiterating railway geometric patterns which lengths over kilometres of spans.

6. Acknowledgements

We express our gratitude to Fugro NL Land B.V. who provided data for evaluation. This research is funded by Cambridge Commonwealth, European & International Trust and Bentley Systems UK Plc. We gratefully acknowledge their support. Any opinions, findings and conclusions expressed in this paper are those of the authors and do not necessarily reflect the views of the institutes mentioned above.

References

Agapaki, E. and Brilakis, I. (2018), "State-of-practice on As-Is Modelling of Industrial Facilities", in Smith, I. and Domer, B. (Eds.), *Advanced Computing Strategies for Engineering. EG-ICE 2018. Lecture Notes in Computer Science*, Springer, Lausanne, Switzerland, available at:https://doi.org/10.1007/978-3-319-91635-4_6.

Arastounia, M. and Elberink, S.O. (2016), "Application of template matching for improving classification of urban railroad point clouds", *Sensors (Switzerland)*, Vol. 16 No. 12, available at:https://doi.org/10.3390/s16122112.

Ariyachandra, M.R.M.F. and Brilakis, I. (2019), "Understanding the challenge of digitally twinning the geometry of existing rail infrastructure", *12th FARU International Research Conference (Faculty of Architecture Research Unit)*, Faculty of Architecture Research Unit, Univeristy of Moratuwa, Colombo, Sri Lanka, pp. 25–32.

Ariyachandra, M.R.M.F. and Brilakis, I. (2020a), "Detection of Railway Masts in Air-Borne LiDAR Data", *Journal of Construction Engineering and Management*, Vol. 146 No. 9, available at:https://doi.org/10.1061/(ASCE)CO.1943-7862.0001894.

Ariyachandra, M.R.M.F. and Brilakis, I. (2020b), "Digital Twinning of Railway Overhead Line Equipment from Airborne LiDAR Data", *Proceedings of the 37th International Symposium on Automation and Robotics in Construction (ISARC)*, pp. 1270–1277.

Ariyachandra, M.R.M.F. and Brilakis, I. (2021), "Application of Railway Topology for the Automated Generation of Geometric Digital Twins of Railway Masts", *Proceedings of the 13th European Conference on Product & Process Modelling*, European Association of Product and Process Modelling (EAPPM), Moscow, Russia, available at:https://doi.org/10.17863/CAM.62196.

Bentley Systems. (2018), *Bentley Systems ' New OpenRail Is First to Advance BIM for the Full Rail*

and Transit Lifecycle.

Borrmann, A. and Berkhahn, V. (2018), *Principles of Geometric Modeling*, edited by Borrmann A., König M., Koch C., B.J., Springer International Publishing AG, available at:https://doi.org/https://doi.org/10.1007/978-3-319-92862-3_2.

Buckley, B. and Logan, K. (2017), *SmartMarket Report The Business Value of BIM for Infrastructure*.

Budroni, A. and Boehm, J. (2010), "Automated 3D Reconstruction of Interiors from Point Clouds", *International Journal of Architectural Computing*, Vol. 8 No. 1, pp. 55–73.

Cheng, Y.J., Qiu, W.G. and Duan, D.Y. (2019), "Automatic creation of as-is building information model from single-track railway tunnel point clouds", *Automation in Construction*, Elsevier, Vol. 106 No. August, available at:https://doi.org/10.1016/j.autcon.2019.102911.

Deng, Y., Cheng, J.C.P. and Anumba, C. (2016), "Mapping between BIM and 3D GIS in different levels of detail using schema mediation and instance comparison", *Automation in Construction*, Vol. 67 No. July, pp. 1–21.

Dvořák, Z., Sventeková, E., Řehák, D. and Čekerevac, Z. (2017), "Assessment of Critical Infrastructure Elements in Transport", *Procedia Engineering*, Vol. 187 No. June, pp. 548–555.

European Commission. (2017), *Technical Specifications for Interoperability Relating to the "infrastructure" Subsystem of the Rail System in the European Union*, Vol. 10, pp. 1–21.

European Railway Agency. (2020), *Report on Railway Safety and Interoperability in the EU*, available at:https://doi.org/10.2821/30980.

Gerbert, P., Castagnino, S., Rothballer, C., Renz, A. and Filitz, R. (2016), *Digital in Engineering and Construction: The Transformative Power of Building Information Modeling*, available at: http://futureofconstruction.org/content/uploads/2016/09/BCG-Digital-in-Engineering-and-Construction-Mar-2016.pdf.

Gézero, L. and Antunes, C. (2019), "Automated three-dimensional linear elements extraction from mobile lidar point clouds in railway environments", *Infrastructures*, Vol. 4 No. 3, available at:https://doi.org/10.3390/infrastructures4030046.

Gradients of the British Main Line Railways. (2016), , Ian Allan Publishing.

Jeon, W.G. and Choi, B.G. (2013), "A study on the automatic detection of railroad power lines using LiDAR data and RANSAC algorithm", *Journal of the Korean Society of Surveying Geodesy Photogrammetry and Cartography*, Vol. 31 No. 4, pp. 331–339.

Jeon, W.G. and Kim, E.M. (2019), "Automated reconstruction of railroad rail using helicopter-borne light detection and ranging in a train station", *Sensors and Materials*, Vol. 31 No. 10, pp. 3289–3302.

Jwa, Y. and Sonh, G. (2015), "Kalman filter based railway tracking from mobile lidar data", *ISPRS Annals of the Photogrammetry, Remote Sensing and Spatial Information Sciences*, Vol. 2 No. 3W5, pp. 159–164.

Kenley, R., Harfield, T. and Behnam, A. (2016), "BIM Interoperability Limitations: Australian and Malaysian Rail Projects", *MATEC Web of Conferences*, Vol. 66, p. 00102.

Koch, C. and Konig, M. (2018), "Data Modeling", *Building Information Modeling*, Springer International Publishing AG, part of Springer Nature 2018, pp. 43–62.

Laefer, D.F. and Truong-hong, L. (2017), "Toward automatic generation of 3D steel structures for building information modelling", *Automation in Construction*, No. November, available at:https://doi.org/10.1016/j.autcon.2016.11.011.

Lee, C.E. (1945), "The World's Oldest Railway", *Transactions of the Newcomen Society*, Vol. 25 No. 1, pp. 141–162.

Limberger, F.A. and Oliveira, M.M. (2015), "Real-time detection of planar regions in unorganized point clouds", *Pattern Recognition*, Elsevier, Vol. 48 No. 6, pp. 2043–2053.

Lou, Y., Zhang, T., Tang, J., Song, W., Zhang, Y. and Chen, L. (2018), "A fast algorithm for rail extraction using mobile laser scanning data", *Remote Sensing*, Vol. 10 No. 12, available at:https://doi.org/10.3390/rs10121998.

Lu, R. and Brilakis, I. (2020), "A benchmarked framework for geometric digital twinning of slab and

beam-and-slab bridges", Vol. 172 No. 2019, pp. 3–18.

Network Rail. (2018), "Catalogue of Network Rail Standards", available at: https://www.networkrail.co.uk/wp-content/uploads/2018/04/Network-Rail-Standards-Catalogue.pdf (accessed 5 January 2019).

Niina, Y., Honma, R., Honma, Y., Kondo, K., Tsuji, K., Hiramatsu, T. and Oketani, E. (2018), "Automatic rail extraction and celarance check with a point cloud captured by MLS in a Railway", *International Archives of the Photogrammetry, Remote Sensing and Spatial Information Sciences - ISPRS Archives*, Vol. 42 No. 2, pp. 767–771.

Oesau, S., Lafarge, F. and Alliez, P. (2014), "Indoor scene reconstruction using feature sensitive primitive extraction and graph-cut", *ISPRS Journal of Photogrammetry and Remote Sensing*, International Society for Photogrammetry and Remote Sensing, Inc. (ISPRS), Vol. 90, pp. 68–82.

Oude Elberink, S., Khoshelham, K., Arastounia, M. and Diaz Benito, D. (2013), "Rail Track Detection and Modelling in Mobile Laser Scanner Data", *ISPRS Annals of Photogrammetry, Remote Sensing and Spatial Information Sciences*, Vol. II-5/W2 No. November, pp. 223–228.

Pastucha, E. (2016), "Catenary system detection, localization and classification using mobile scanning data", *Remote Sensing*, Vol. 8 No. 10, available at:https://doi.org/10.3390/rs8100801.

Patil, A.K., Holi, P., Lee, S.K. and Chai, Y.H. (2017), "An adaptive approach for the reconstruction and modeling of as-built 3D pipelines from point clouds Automation in Construction An adaptive approach for the reconstruction and modeling of as-built 3D pipelines from point clouds", *Automation in Construction*, Elsevier B.V., Vol. 75 No. November 2018, pp. 65–78.

Rail Delivery Group. (2014), *What Is the Contribution of Rail to the UK Economy?*, available at: https://www.oxera.com/wp-content/uploads/2018/07/Contribution-of-rail-to-the-UK-economy-140714.pdf.pdf.

RailEngineer. (2020), *Why Rail Electrification Is Key?*

Rusu, R.B., Marton, Z.C., Blodow, N., Dolha, M. and Beetz, M. (2008), "Towards 3D Point cloud based object maps for household environments", *Robotics and Autonomous Systems*, Elsevier B.V., Vol. 56 No. 11, pp. 927–941.

Sacks, R., Ma, L., Yosef, R., Borrmann, A., Daum, S. and Kattel, U. (2017), "Semantic Enrichment for Building Information Modeling: Procedure for Compiling Inference Rules and Operators for Complex Geometry", *Journal of Computing in Civil Engineering*, Vol. 31 No. 6, p. 04017062.

Sánchez-Rodríguez, A., Riveiro, B., Soilán, M. and González-deSantos, L.M. (2018), "Automated detection and decomposition of railway tunnels from Mobile Laser Scanning Datasets", *Automation in Construction*, Elsevier, Vol. 96 No. April, pp. 171–179.

Schnabel, R., Wahl, R. and Klein, R. (2007), "Efficient RANSAC for Point-Cloud Shape Detection", *Computer Graphics Forum*, Vol. 26 No. 2, pp. 214–226.

Soni, A. (2016), *Non-Contact Monitoring of Railway Infrastructure with Terrestrial Laser Scanning and Photogrammetry at Network Rail*, available at: https://discovery.ucl.ac.uk/id/eprint/1477352/.

Valero, E. and Cerrada, C. (2012), "Automatic Method for Building Indoor Boundary Models from Dense Point Clouds Collected by Laser Scanners", *Sensors*, Vol. 12, pp. 16099–16115.

Wilson, J.R., Farrington-Darby, T., Cox, G., Bye, R. and Hockey, G.R.J. (2007), "The railway as a socio-technical system: Human factors at the heart of successful rail engineering", *Proceedings of the Institution of Mechanical Engineers, Part F: Journal of Rail and Rapid Transit*, Vol. 221 No. 1, pp. 101–115.

Xiao, J. and Furukawa, Y. (2012), "Reconstructing the World ' s Museums", *International Journal of Computer Vision*, Vol. 110 No. 3, pp. 668–681.

Yang, B. and Fang, L. (2014), "Automated Extraction of 3-D Railway Tracks from Mobile Laser Scanning Point Clouds", *IEEE Journal of Selected Topics in Applied Earth Observations and Remote Sensing*, Vol. 7 No. 12, pp. 1–12.

Zio, E. (2018), "The future of risk assessment", *Reliability Engineering and System Safety*, Elsevier Ltd, Vol. 177 No. June 2017, pp. 176–190.